Seismic Retrofit of a Cable-Stayed Bridge with Passive Control Techniques: A Comparative Investigation through Non-Linear Dynamic Analyses

M.D. Martínez-Rodrigo
Mechanical Engineering and Construction Department, Universitat Jaume I, Castellón, Spain

A. Filiatrault
Department. of Civil, Structural and Environmental Engineering, State University of New York at Buffalo, USA

15 WCEE
LISBOA 2012

SUMMARY:
The present contribution deals with the seismic performance of an existing cable-stayed steel bridge. The structure experienced damage during the Saguenay earthquake in 1988 needing structural rehabilitation. As an alternative, in this study the retrofit of the structure with different passive supplemental damping and seismic isolation systems is proposed and evaluated in order to achieve an admissible performance of the bridge under a set of seismic events of different magnitudes including near field records. To this end a Finite Element numerical planar model is implemented and the bridge response is obtained trough non-linear dynamic analyses. Strength degradation capabilities are included in the model allowing the occurrence of brittle failure when certain levels of ductility are exceeded in the members. The major improvement in the overall response of the bridge is shown and conclusions regarding the most appropriate retrofit alternative for the particular case are derived.

Keywords: Cable stayed bridge, seismic retrofit, passive control, seismic isolation, non-linear dynamic analysis

1. INTRODUCTION

This study deals with the seismic performance and possible retrofit of the existing steel Shipshaw Bridge, crossing the Saguenay river near Jonquière, Quebec, Canada (Fig. 1). The structure was damaged during the November 25th 1988, Saguenay earthquake. As a consequence of this event one of the four anchorage plates connecting the steel girders to one of the abutments completely failed which lead to the closing of the infrastructure for a short period and its subsequent repair (Filiatrault 1993a, 1993b).

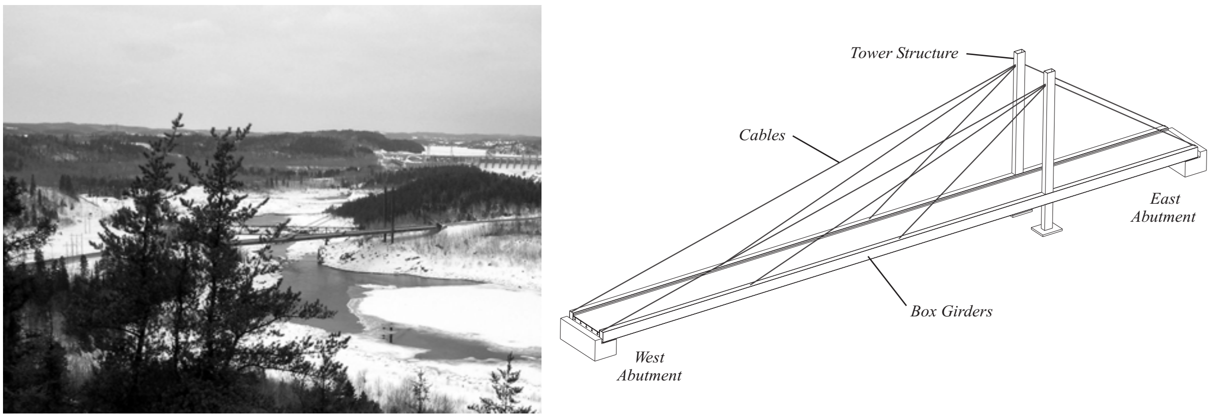

Figure 1. Shipshaw bridge surroundings and structural scheme

In this study, the possibility of retrofitting the structure applying supplemental damping and seismic isolation systems is addressed as an alternative. In particular, the retrofit of the bridge is considered based on Hysteretic Dampers, Fluid Viscous Dampers, Tuned Mass Dampers and a Friction Pendulum

System. The main objective of the investigation is to evaluate how these innovative techniques are able to improve the bridge response in terms of reducing the yielding levels and mitigating the vibratory regime. Based on these results it will be possible to assess what retrofitting system results in a better alternative for the selected set of earthquake records.

2. BRIDGE STRUCTURE AND NUMERICAL MODEL DESCRIPTION

The bridge under study consists of a double leg steel tower, double-plane fan-type cables and two steel box girders supporting a composite concrete steel deck. The bridge total length is 183 m divided into four identical spans between the abutments and the cable anchorages (see Fig. 2). There is a 4% upward slope from the west to the east abutment along the deck.

The bridge deck is composed of a 165 mm concrete slab, 110 m wide, with two non-structural precast parapets. Five longitudinal steel stringers are spaced at equal transverse intervals of 2.4 m. Floor beams, transverse to the main girders at equally spaced intervals of 7 m, transfer stringer loads to the two main box girders at the outer edges of the deck. The 1.5 x 3 m box girders are made of welded flanges, webs, stiffeners and diaphragms. The cables are connected to the deck at the top flange of the main box girders. The tower, consists of two 1.5 x 2.4 m rectangular box steel legs and a cross beam supporting the deck. The top of the tower is 43 m tall. The thickness of the flanges and webs of the box steel legs and the box girder equal 50 mm. Each leg of the tower is rigidly connected to the intersecting box girder at the deck level.

The support system of the bridge is assumed to be founded on rock. At each of the abutments there are roller supports resisting the uplift forces generated by the cables, which allow for sliding in the longitudinal direction of the bridge. The bearings under each leg of the tower prevent horizontal and vertical movements and permit rotation around the transverse axis of the bridge only. The bridge incorporates 4 cables per tower each composed of 9 strands. Each strand has a cross-sectional area of 65.1 mm^2. The cables are constructed from standard galvanized bridge strands with a Young's modulus of 175 GPa, yield strength of 1500 MPa and ultimate strength of 1725 MPa. A full description of the bridge structure under study may be found in Christopoulos and Filiatrault (2006).

The dynamic response of the bridge structure under the action of a series of ground motions is investigated through numerical analyses. To this end a Finite Element (FE) numerical model of the bridge is implemented using the nonlinear dynamic analysis computer program RUAUMOKO (Carr 2002). As only horizontal ground excitation is considered and the structure is symmetrical only half of the bridge is modeled (see Fig. 2). Therefore the model includes one main box girder, representing the deck discretized in 19 frame elements, one tower box girder (13 frame elements) and 4 sets of cables modeled as tension-only truss elements. The concrete deck, steel stringers and floor beams are considered rigid and its dead load (25 kN/m for half of the bridge) is applied to the girder.

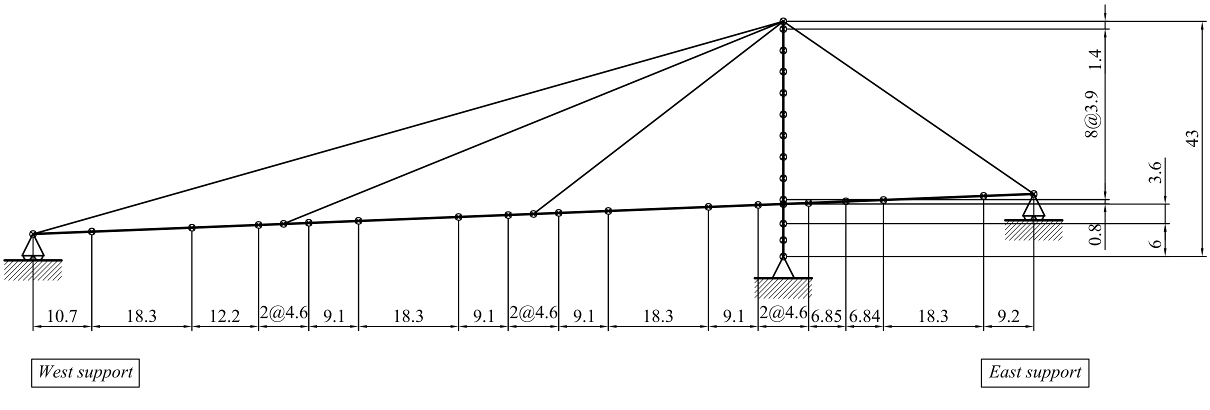

Figure 2. Bridge structure model

The inelastic flexural response of the box girder and the tower is concentrated in plastic hinges that could form at the end of the frame elements. These hinges are assigned a bi-linear hysteretic behavior with a curvature strain-hardening ratio of 0.02 (see Fig. 3a). The hinges' length is set equal to 90% of the member depth. The plastic resistance of the hinges is based on the expected yield strength of 290 MPa. An axial load-moment interaction (AISC 1993) is considered for the tower elements. The inelastic tensile response of the cables is modeled with a tension-only bi-linear hysteretic behavior (see Fig. 3b). The tensile strain-hardening ratio is set to 0.1. In all the elements the possible occurrence of brittle failure has been introduced by forcing the sudden degradation of the member strength after the ultimate curvature ductility or elongation ductility demands have been exceeded, as it is shown in Fig. 3 for both frame and cable elements.

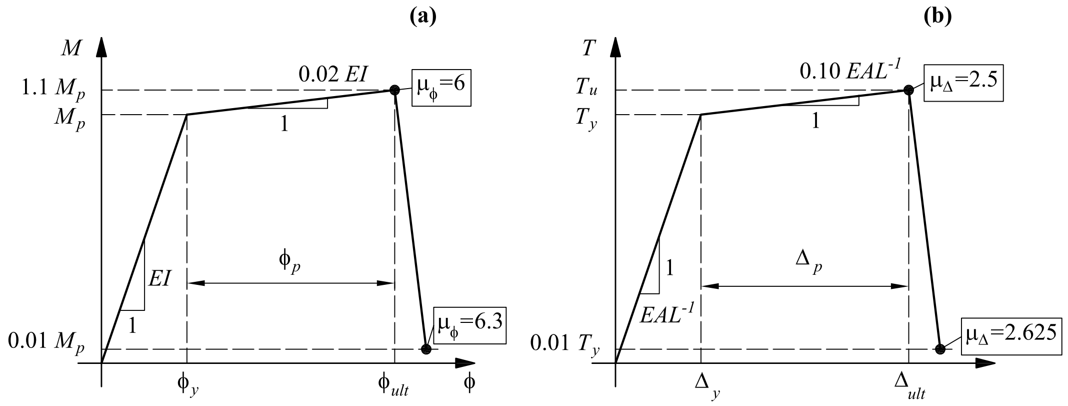

Figure 3. Bi-linear (a) moment-curvature model for girder and tower and (b) tensile force-elongation model for cables

Figure 4 shows the deformed shape of the bridge girder and the tower in the first elastic six modes of vibration computed with the previously described FE model. The first six undamped natural periods of the structure are also included in Fig. 4b.

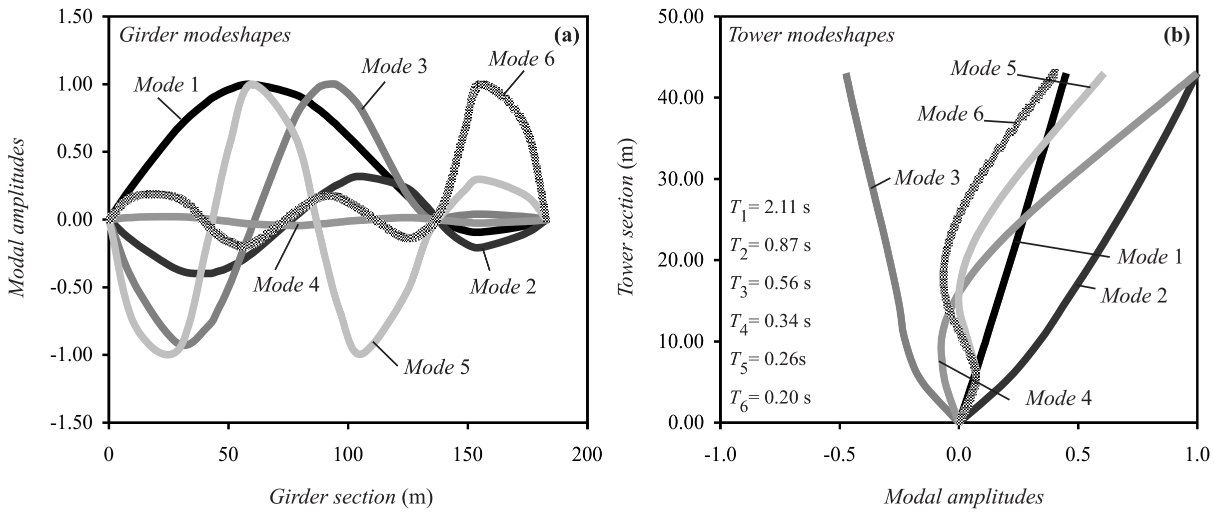

Figure 4. Deformed shape of (a) the box girder and (b) the tower in the first six modes of vibration. First six natural periods

Finally, for the subsequent dynamic analyses (i) Rayleigh damping of 1% based on the first two modes of vibration of the structure is assumed; and (ii) the equations of motion are integrated in the time domain using the Newmark Constant Average Acceleration numerical integration scheme.

3. INPUT GROUND MOTIONS

In order to analyze the dynamic performance of the bridge and investigate the possibility of retrofitting the structure, 21 ground motions recorded during the Imperial Valley 1940, Landers 1992, Loma Prieta 1989, Northridge 1994 and North Palm Springs 1996 earthquakes are considered. Table 1 summarizes the main features of these records. Records LA01 to LA20 are related to regular (far-field) events with peak ground accelerations ranging from 0.23 to 1.02g, while NF13 corresponds to a near field record characterized by a strong ground acceleration pulse.

File	Ground motion	Station	Dir	Duration (s)	pga (g)
LA01	Imperial Valley 1940	EC Valley Irr Dist	fn	53.46	0.46
LA02	Imperial Valley 1940	EC Valley Irr Dist	fp	53.46	0.68
LA03	Imperial Valley 1940	EC Array 5 James Road	fn	39.38	0.39
LA04	Imperial Valley 1940	EC Array 5 James Road	fp	39.38	0.49
LA05	Imperial Valley 1940	EC Array 6 Houston Road	fn	39.08	0.30
LA06	Imperial Valley 1940	EC Array 6 Houston Road	fp	39.08	0.23
LA07	Landers 1992	Barstow-Vineyard & H	fn	79.98	0.42
LA08	Landers 1992	Barstow-Vineyard & H	fp	79.98	0.43
LA09	Landers 1992	Yermo Fire Station	fn	79.98	0.52
LA10	Landers 1992	Yermo Fire Station	fp	79.98	0.36
LA11	Loma Prieta 1989	Gilroy Sewage plant	fn	39.98	0.67
LA12	Loma Prieta 1989	Gilroy Sewage plant	fp	39.98	0.97
LA13	Northridge 1994	County Fire Station	fn	59.98	0.68
LA14	Northridge 1994	County Fire Station	fp	59.98	0.66
LA15	Northridge 1994	Rinaldi Receiving Station	fn	14.95	0.53
LA16	Northridge 1994	Rinaldi Receiving Station	fp	14.95	0.58
LA17	Northridge 1994	Sylmar, Olive View	fn	59.98	0.57
LA18	Northridge 1994	Sylmar, Olive View	fp	59.98	0.82
LA19	North Palm Springs 1986	North Palm Springs 1986	fn	59.98	1.02
LA20	North Palm Springs 1986	North Palm Springs 1986	fp	59.98	0.99
NF13	Northridge 1994	Rinaldi Receiving Station	fn	14.95	0.89

Table 1. Earthquake records features

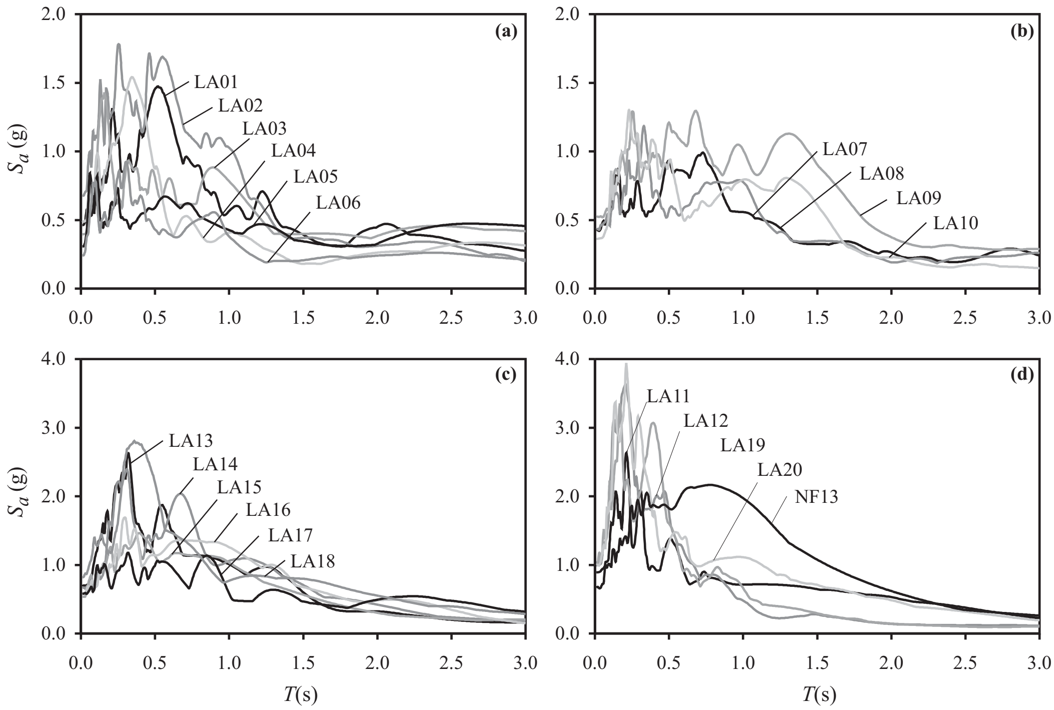

Figure 5. Absolute acceleration response spectra (5% damping) for the 21 earthquake records

In order to get some insight of the frequency distribution of the seismic energy associated to the events under consideration, exact elastic absolute acceleration spectra have been plotted for 5% damping, as shown in Fig. 5. The performance of the bridge is presented and analyzed under the horizontal action of these 21 records. Therefore, no vertical seismic input is considered in this study.

4. ORIGINAL STRUCTURE DYNAMIC PERFORMANCE

In this section the dynamic performance of the structure is presented in its original condition (before retrofit). In what follows the structure performance will be compared before and after the retrofit in terms of the maximum ductility demand experienced by its members and maximum absolute acceleration at the tower top. Ductility demand is defined as follows for the girder and tower elements and for the cable sets:

$$\mu_\phi = \left(\phi_p - \phi_y\right)\cdot\phi_y^{-1} \qquad \mu_\Delta = \left(\Delta_p - \Delta_y\right)\cdot\Delta_y^{-1} \tag{4.1}$$

where ϕ_y and ϕ_p are the yielding and plastic curvature in the frame elements, respectively, and Δ_y and Δ_p are the yielding and plastic elongation in the cables. Maximum levels of relative displacement are checked as well in all the scenarios but may not be included for the sake of briefness. First, the original bridge structure dynamic response is obtained under the horizontal action of the 21 earthquake records described in the previous section. Table 2 summarizes the maximum curvature ductility demands attained in the box-girder, tower and cable elements along with the particular element where this maximum ductility takes place (see Fig. 6). The structure remains elastic only under the action of the LA04 ground motion, it experiences severe yielding under many of the remaining earthquakes and collapses under the near field record. Yielding mainly concentrates in the junction between the box girder and the tower (elements 14, 15 and 30 which have been indicated in Fig. 6). Apart from the NF13 record, the highest curvature ductility demand reaches 4.49 (6 being the ultimate curvature ductility in the girder and the tower hinges) under the LA16 record. Regarding the cables, the maximum ductility reaches 1.68 in cable E36 (2.5 being the ultimate ductility demand right before strength degradation conditions are applied (see Fig. 3b).

Record	$\lvert\mu_{max}\rvert$ girder	$\lvert\mu_{max}\rvert$ tower	μ_{max} cable	Record	$\lvert\mu_{max}\rvert$ girder	$\lvert\mu_{max}\rvert$ tower	μ_{max} cable
LA01	2.88-E15	---	1.35-E36	**LA12**	2.85-E14	1.04E30	1.28-E36
LA02	4.22-E15	1.95-E30	1.68-E36	**LA13**	3.68-E14	---	1.21-E35
LA03	3.53-E15	1.03-E30	1.42-E36	**LA14**	3.23-E15	---	1.49-E36
LA04	---	---	---	**LA15**	3.87-E15	---	1.52-E36
LA05	1.43-E15	---	---	**LA16**	4.49-E15	---	1.68-E36
LA06	2.45-E15	---	1.22-E36	**LA17**	3.97-E15	---	1.54-E36
LA07	2.06-E15	---	1.13-E36	**LA18**	2.29-E15	1.02-E30	1.31-E36
LA08	2.40-E15	---	1.27-E36	**LA19**	3.86-E15	1.27-E30	1.52-E36
LA09	2.79-E15	---	1.37-E36	**LA20**	3.50-E15	---	1.49-E36
LA10	3.01-E15	---	1.30-E36	**NF13**	**COLLAPSE**		
LA11	2.01-E15	---	1.15-E36				

Table 2. Maximum ductility demands in the unretrofitted case

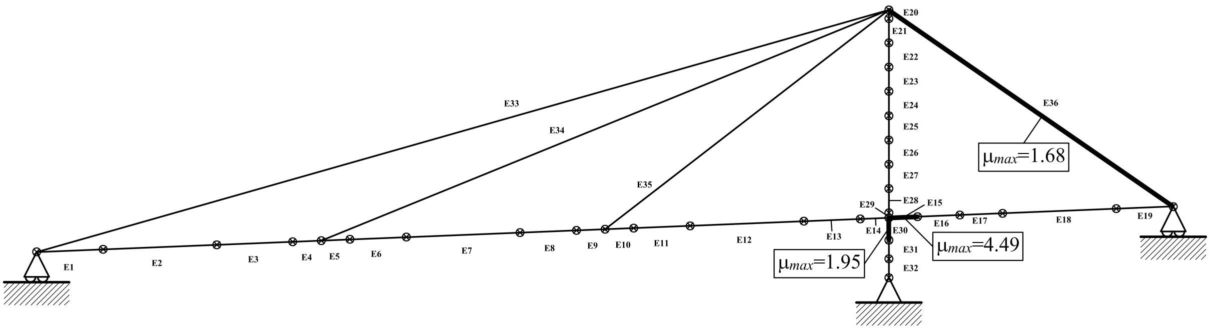

Figure 6. Elements with maximum ductility demands in box-girder, tower and cables

Figure 7 shows the horizontal absolute acceleration time-history of the top of the tower (black line) in the LA16 case, which leads to the maximum level of curvature ductility demand after the near field record, has been represented. In the next sections different passive control and base isolation strategies are proposed and designed with the aim of reducing as much as possible the yielding in the structure under the records LA01 to LA20 and preventing the collapse under the near field event.

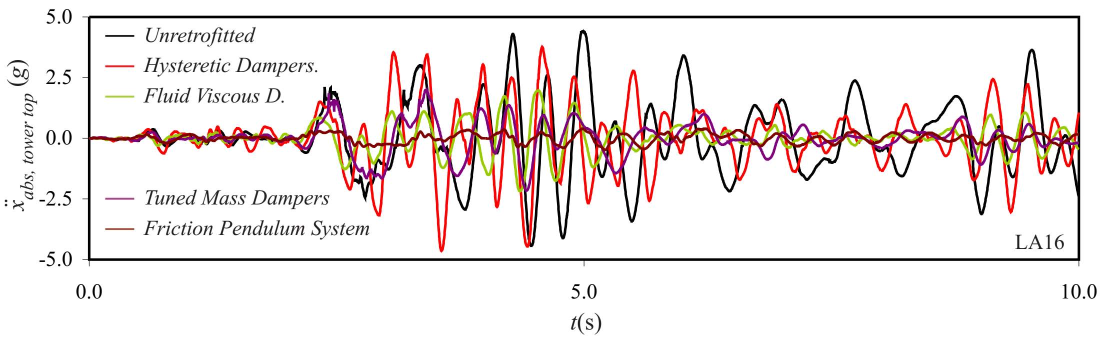

Figure 7. Absolute horizontal acceleration of the top of the tower under LA16

5. RETROFIT WITH HYSTERETIC DAMPERS

The first passive control strategy considered is the retrofit with Hysteretic Dampers (HD) (metallic or friction dampers), which belong to the category of displacement-activated supplemental damping devices. As the horizontal displacements of the roller supports should not be prevented under traffic loads or thermal variations the devices cannot be installed between the box girder and the abutments. Furthermore, as in the unretrofitted case, yielding mainly concentrates around the girder-tower junction it is proposed to introduce two HD connecting the base of the tower with the box girder as shown in Fig. 8. The brace and the damper itself are modeled by means of a one-dimensional spring element with an elastic-perfectly plastic load-displacement relationship, both in tension and in compression, as that shown in Fig. 8. In this figure, F_a and $\bar{k}$ are the activation load and the elastic axial stiffness of the braces, respectively. In general stiffer braces lead to better results allowing lowering the ductility demand in the most unfavorable elements.

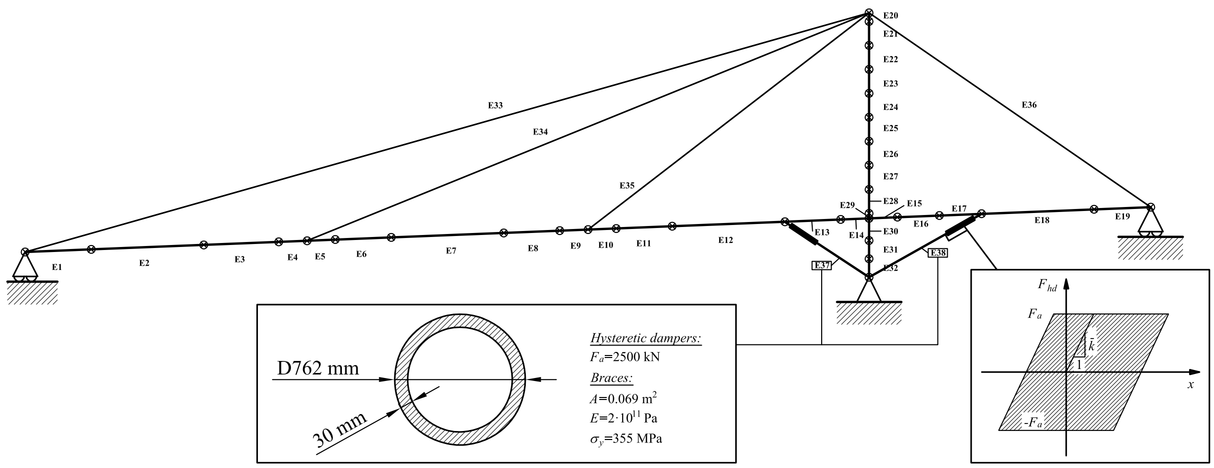

Figure 8. Retrofit with Hysteretic Dampers. Final configuration and design

The activation load of the dampers (or yield load of the spring) is selected in order to minimize the maximum ductility demand under seismic event LA16, which led to the highest ductility values except for de near field record. It is observed that for low values of the slip load the box-girder yields. As F_a increases ductility demands in the girder decrease, but after a certain point the tower starts to yield close to the junction with the beam. The load leading to the minimum ductility in the girder elements while still preventing yielding in the tower is considered to be the optimum activation load. The final design selected for the braces and the dampers is also shown in Fig. 8. Other possibilities obtained by varying the inclination angle of the braces have been investigated and it finally has been concluded that the one presented herein leads to a better structural response with smaller sizes of the braces.

Table 3 shows the maximum ductility demands attained after the retrofit with HDs. The collapse of the structure is prevented under the near field record. The maximum ductility demand in the girder reaches 2.44 in this particular case. The tower does not yield under any of the ground motions and the maximum level of ductility in the cables is 1.36. The structure remains elastic under the action of nine out of the 21 evaluated records and the maximum curvature ductility in the box-girder is lower than 2 in all the cases except for LA14 and NF13. The improvement in the structural performance with the HD based retrofit is evident.

Record	$\lvert\mu_{max}\rvert$ girder	$\lvert\mu_{max}\rvert$ tower	μ_{max} cable	Record	$\lvert\mu_{max}\rvert$ girder	$\lvert\mu_{max}\rvert$ tower	μ_{max} cable
LA01	---	---	1.01-E36	**LA12**	1.26-E14	---	1.05-E36
LA02	1.01-E15	---	---	**LA13**	1.16-E14	---	1.05-E36
LA03	---	---	---	**LA14**	2.06-E15	---	1.23-E36
LA04	---	---	---	**LA15**	---	---	1.04-E36
LA05	---	---	---	**LA16**	---	---	---
LA06	---	---	---	**LA17**	---	---	---
LA07	---	---	---	**LA18**	1.49-E14	---	---
LA08	---	---	---	**LA19**	1.24-E14	---	1.07-E36
LA09	1.02-E15	---	---	**LA20**	1.06-E14	---	1.11-E36
LA10	---	---	---	**NF13**	2.44-E15	---	1.31-E36
LA11	1.04-E14	---	1.02-E36				

Table 3. Retrofit with Hysteretic Dampers. Maximum ductility demands attained

As possible drawbacks of this alternative it may be said that this solution requires large brace sections. In this case steel hollow circular tubes of 762 mm of external diameter and 30 mm of thickness are needed as the elements are considerably slender and compression loads are important. Also the level of accelerations in the top of the tower is not reduced substantially, as shown in Fig. 7.

6. RETROFIT WITH FLUID VISCOUS DAMPERS

As a second alternative the possibility of retrofitting the structure with linear Fluid Viscous Dampers (FVD) is considered. The proposed design consists of connecting two pure viscous elements between the box girder and the abutments as shown in Fig. 9. As these elements do not exert any force under static loads, they should not prevent the roller supports horizontal movement associated to service loads or thermal dilatations. The retrofit with pure viscous elements should lead to an increase of the overall damping of the bridge without modification of its stiffness and therefore of its dynamic characteristics. In a practical application the dampers would connect the abutments with some point of the box girder, nevertheless, the model represented in Fig. 9 is evaluated as a first approach.

In order to select the most appropriate FVD constants, the Near Field ground motion record NF13 is used this time as the expected improvement in the performance is higher than in the previous case. The behavior of the retrofitted structure is evaluated considering progressively increasing values of the dampers constants (in 500 kN increments). As the dampers constant increase the bridge response monotonically decreases and the performance in terms of maximum ductility demands considerably improves. Therefore the minimum dampers constants leading to the desired structural performance have been selected taking into account that the maximum force in the dampers also increases with the dampers constants. Finally a similar viscous damping constant in both devices of C_D=13500 kNs/m was selected. Exceeding this constant value, the improvement in the performance is very marginal and the dampers forces increase rapidly. The bridge response retrofitted with these dampers is evaluated under the rest of the ground motions.

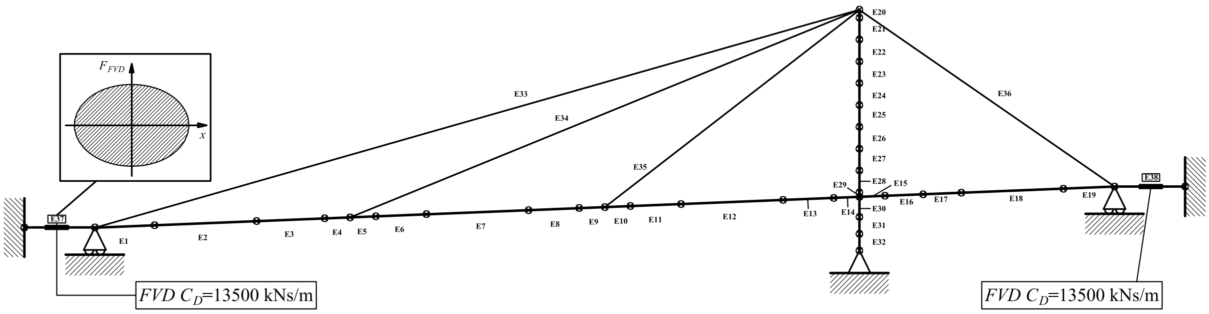

Figure 9. Retrofit with Fluid Viscous Dampers. Final configuration and design

After the retrofit the structure remains elastic under all the ground motions (including the near field) with the exception of the LA18 record (μ_{max}=1.24 in element 14). The maximum force experienced by the most unfavorable damper reaches 4804 kN and takes place under the near field record. Regarding the levels of horizontal acceleration as it can be observed in Fig. 7, the retrofit with viscous dampers drastically reduces the absolute acceleration of the top of the tower. The maximum value in the unretrofitted case is reduced in fact by 50%. This fact is consistent with the increment of overall damping that the devices induce into the structure with almost no other modification. One of the advantages of this alternative, aside from the performance improvement itself, is that no braces (or not long braces) are needed to connect the dampers to the abutments.

7. RETROFIT WITH TUNED MASS DAMPER

The next structural modification considered in order to improve the seismic performance of the bridge is the addition of Tuned Mass Dampers (TMD). These elements are relatively small mass-spring dashpot systems calibrated to be in resonance with a particular mode of the structure on which they are installed. In Fig. 4 it can be observed that in the first mode of vibration the most significant deformations are experienced by the box-girder while in the second mode the tower deforms to a larger extent. For this reason it is decided to install one TMD with horizontal movement connected to the top of the tower (see Fig. 10), tuned to the second natural frequency (1.15 Hz). The effect of, installing a second vertical damper connected to the girder and tuned to the fundamental frequency was checked but its influence in improving the dynamic of the bridge was negligible.

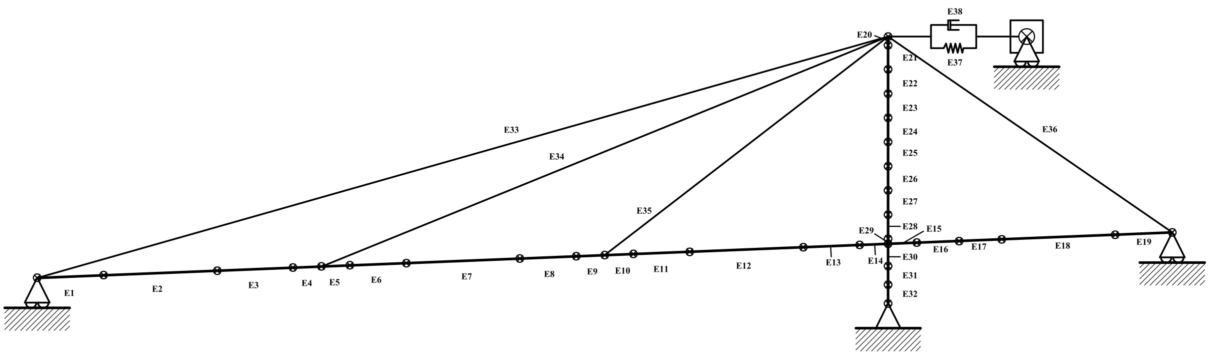

Figure 10. Retrofit with tuned mass damper

The optimum tuning conditions (frequency and damping) for the TMD are obtained by fixing the value of the mass ratio between the TMD mass and the second modal mass of the structure and applying the optimal conditions for random input (Constantinou et. al., 1998), i.e.:

$$\eta = \sqrt{1-\frac{\mu}{2}} \Big/ (1+\mu) \qquad\qquad c/c_c = \sqrt{\mu\left(1+\frac{3\mu}{4}\right) \Big/ 4(1+\mu)\left(1-\frac{\mu}{2}\right)} \tag{7.1}$$

being μ and η the mass and frequency ratios between the TMD and the unretrofitted bridge second modal mass and frequency, and c/c_c is the viscous damping ratio of the TMD, respectively. In order to select the most appropriate mass ratio for the TMD, a preliminary parametric analysis is performed and the bridge response in terms of maximum ductility demand is obtained for different mass ratios under the LA16 record. It is detected that from μ=0.01 up to μ=0.20 the structure maximum ductility demands monotonically reduce with the mass of the TMD. For practical reasons it is decided not to increase the mass ratio over μ=0.20 and this value is finally selected. For the designed TMD the volume needed of a concrete block with a cubical shape considering a mass density of 2500 kg/m^3 would be 2.68×2.68×2.68 m^3.

Once the TMD is designed the performance of the structure under the action of the remaining ground motions is obtained. The structure remains elastic under 9 out of the 21 records and almost elastic under 5 additional ones. Collapse is prevented under the near field record leading to a maximum curvature ductility of 2.44 in the box girder. The improvement of the structure performance is evident leading to a reduction in the top of the tower horizontal acceleration of about 50%, as shown in Fig. 7. The system could be embodied in a pendulum system hanging from a transverse girder linking both halves of the bridge. Nevertheless the size of the required mass to achieve the above mentioned performance is considerably large.

Record	$\|\mu_{max}\|$ girder	$\|\mu_{max}\|$ tower	μ_{max} cable	Record	$\|\mu_{max}\|$ girder	$\|\mu_{max}\|$ tower	μ_{max} cable
LA01	---	---	1.01-E36	**LA12**	1.26-E14	---	1.05-E36
LA02	1.01-E15	---	---	**LA13**	1.16-E14	---	1.05-E36
LA03	---	---	---	**LA14**	2.06-E15	---	1.23-E36
LA04	---	---	---	**LA15**	---	---	1.04-E36
LA05	---	---	---	**LA16**	---	---	---
LA06	---	---	---	**LA17**	---	---	---
LA07	---	---	---	**LA18**	1.49-E14	---	---
LA08	---	---	---	**LA19**	1.24-E14	---	1.07-E36
LA09	1.02-E15	---	---	**LA20**	1.06-E14	---	1.11-E36
LA10	---	---	---	**NF13**	2.44-E15	---	1.31-E36
LA11	1.04-E14	---	1.02-E36				

Table 4. Retrofit with Tuned Mass damper. Maximum ductility demands attained

8. SEISMIC ISOLATION

As a final retrofit alternative, the possibility of transforming the original structure into an isolated system is considered. To this end the bridge girder is disconnected from the tower column and a Friction Pendulum System (FPS) is introduced between both elements. The tower pier is fixed at the foundation. A FPS is a friction type sliding bearing that uses gravity as the restoring force. An articulated friction slider should be introduced at the location of node 15, which would travel on a spherical concave lining surface introduced at the pier top (node 34). The coefficient of friction μ is set to 0.05. The FPS is modeled as a horizontal spring element with a bilinear hysteretic behavior. A very high value of the initial horizontal stiffness, k_0=10^6 kN/m is provided trying to reproduce the response of a rigid friction spring (see Fig. 11). The yielding force and the post-yielding stiffness are computed in terms of the weight that the FPS supports W=9.98 MN, and R the radius of the lining surface which is set to 1 m. In addition to minimizing the yielding levels in the structure, in this case the maximum seismic displacement of the friction pendulum isolator is limited to ±300 mm in order to avoid pounding between the deck and the abutment. To increase damping and reduce this displacement, linear viscous dampers are also inserted next to the friction pendulum connecting the tower pier and the deck. The damping constants are selected for the particular FPS to reduce the maximum displacement below the limitation (C_D=6000 kN/m).

The seismic response of the bridge clearly improves with the isolation and all the structural members remain elastic even under the near field record. The maximum displacement of the FPS reaches 264 mm below the limitation of ±300 mm. Furthermore the level of maximum accelerations reduces in a 90% with respect to the unretrofitted case.

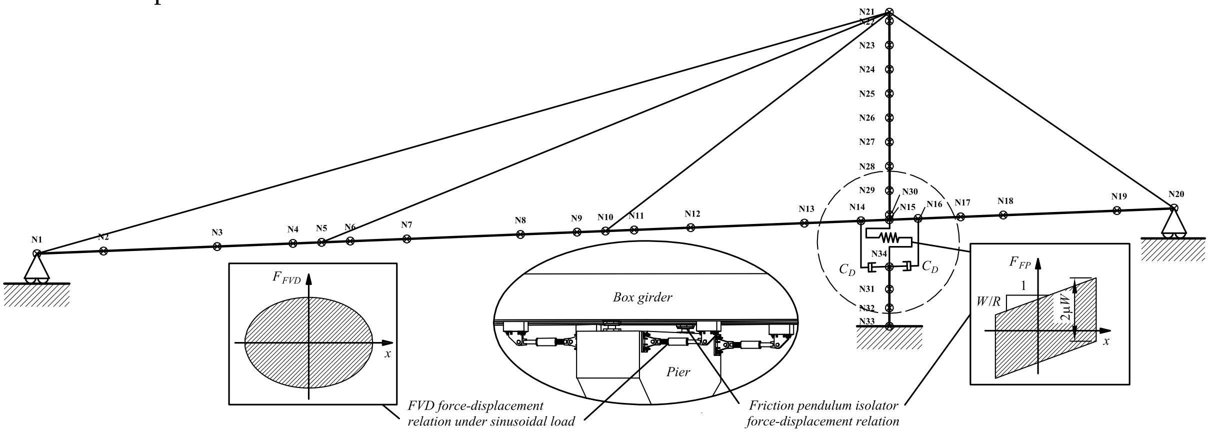

Figure 11. Bridge structure with Friction Pendulum Isolation system scheme

8. CONCLUSIONS

The possible retrofit with supplemental and base isolation systems of an existing cable-stayed bridge damaged during the 1988 Saguenay earthquake is investigated through non-linear dynamic analyses. The effects of introducing in the structure Hysteretic, Viscous, Tuned Mass Dampers and a Friction Pendulum System are compared under the horizontal action of 21 records including a near field event. The structure collapses in the unretrofitted case under the near field record and experiences very important levels of yielding under the remaining ones. All the alternatives prevent the collapse of the bridge and reduce to a great extent the maximum level of ductility demand attained. The structure remains elastic (or almost elastic) under all the records when the FPS is introduced and when retrofitted with FVD. The retrofit with HD leads to an important reduction of yielding in the bridge but less drastic than in the previous two cases. The effectiveness of introducing a TMD is much lower than the remaining alternatives in this regard. When it comes to the maximum horizontal acceleration levels in the top of the tower, these are reduced by about 90% when the structure is base isolated, and close to 50% in the case of retrofitting the bridge with FVD or TMD and are almost not reduced when introducing HD into the bridge. From a practical perspective the retrofit with HD requires the installation of very large size braces and the TMD needed size could complicate its construction. Based on these premises it is concluded that retrofitting the bridge with FVD or introducing a FPS could lead to a major improve in the structural performance and these could be the most appropriate alternatives.

AKCNOWLEDGEMENT

The authors express their gratitude to the Spanish Ministry of Science and Innovation (Ministerio de Ciencia e Innovación, MICINN), for the financial support received in the framework of the Program “*José Castillejo*” with reference number JC2011-0340 for mobility of researchers.

REFERENCES

Filiatrault, A., Tinawi, R., and Massicotte, B. (1993a). Damage to cable-stayed bridge during 1988 Saguenay earthquake I: Pseudostatic analysis. *Journal of Structural Engineering* **119:5**,1432-1449.

Filiatrault, A., Tinawi R., and Massicotte, B. (1993b). Damage to cable-stayed bridge during 1988 Saguenay earthquake I: Dynamic anaysis. *Journal of Structural Engineering* **119:5**,1450-1463.

Christopoulos, C., and Filiatrault, A. (2006). Principles of passive supplemental damping and seismic isolation, IUSS Press, Pavia, Italy.

Carr, A.J. (2002). RUAUMOKO-Inelastic dynamic analysis program, University of Canterbury, Christchurch, New Zealand.

AISC (1993). Load and resistance factor design specifications for structural buildings, American Institute of Steel Construction, Inc., Chicago, IL, USA.

Constantinou, M.C., Soon, T.T., and Dargush, G.F. (1998). Passive energy dissipation systems for structural design and retrofit. MCEER Monograph No. 1, Multidisciplinary Center for Earthquake Engineering Research, Buffalo, NY.